

# Dark Matter Interpretation of the *Fermi*-LAT Observations Toward the Outer Halo of M31

with Simona Murgia,  
Igor Moskalenko,  
Sean Fillingham,  
Anne-Katherine Burns,  
and Max Fieg

Chris Karwin  
Clemson University  
Particles and Nuclei International Conference (PANIC)  
September 8, 2021



# Based on

THE ASTROPHYSICAL JOURNAL, 880:95 (48pp), 2019 August 1

© 2019. The American Astronomical Society. All rights reserved.

<https://doi.org/10.3847/1538-4357/ab2880>



## *Fermi*-LAT Observations of $\gamma$ -Ray Emission toward the Outer Halo of M31

Christopher M. Karwin<sup>1</sup> , Simona Murgia<sup>1</sup> , Sheldon Campbell<sup>1</sup>, and Igor V. Moskalenko<sup>2</sup> 






<sup>1</sup>Department of Physics and Astronomy, University of California, Irvine, CA 92697, USA; [ckarwin@uci.edu](mailto:ckarwin@uci.edu), [smurgia@uci.edu](mailto:smurgia@uci.edu)

<sup>2</sup>Hansen Experimental Physics Laboratory and Kavli Institute for Particle Astrophysics and Cosmology, Stanford University, Stanford, CA 94305, USA  
[imos@stanford.edu](mailto:imos@stanford.edu)

*Received 2019 March 19; revised 2019 June 7; accepted 2019 June 8; published 2019 July 30*

PHYSICAL REVIEW D **103**, 023027 (2021)

## Dark matter interpretation of the *Fermi*-LAT observations toward the outer halo of M31

Christopher M. Karwin<sup>1,2,\*</sup> , Simona Murgia<sup>1,2,†</sup> , Igor V. Moskalenko<sup>1,3,‡</sup> , Sean P. Fillingham<sup>4,2</sup>,  
Anne-Katherine Burns<sup>1,2</sup> , and Max Fieg<sup>1,2</sup> 

<sup>1</sup>Department of Physics and Astronomy, Clemson University, Clemson, South Carolina 29634, USA

<sup>2</sup>Department of Physics and Astronomy, University of California, Irvine, California 92697, USA

<sup>3</sup>Hansen Experimental Physics Laboratory and Kavli Institute for Particle Astrophysics and Cosmology,  
Stanford University, Stanford, California 94035, USA

<sup>4</sup>Department of Astronomy, University of Washington, Seattle, Washington 98105, USA



(Received 9 October 2020; accepted 22 December 2020; published 29 January 2021)

# Outline

---

- Big picture of the MW-M31 System
- Fermi-LAT observations toward M31's outer halo
- Dark matter interpretation
- Summary and Conclusion

# M31's Inner Galaxy

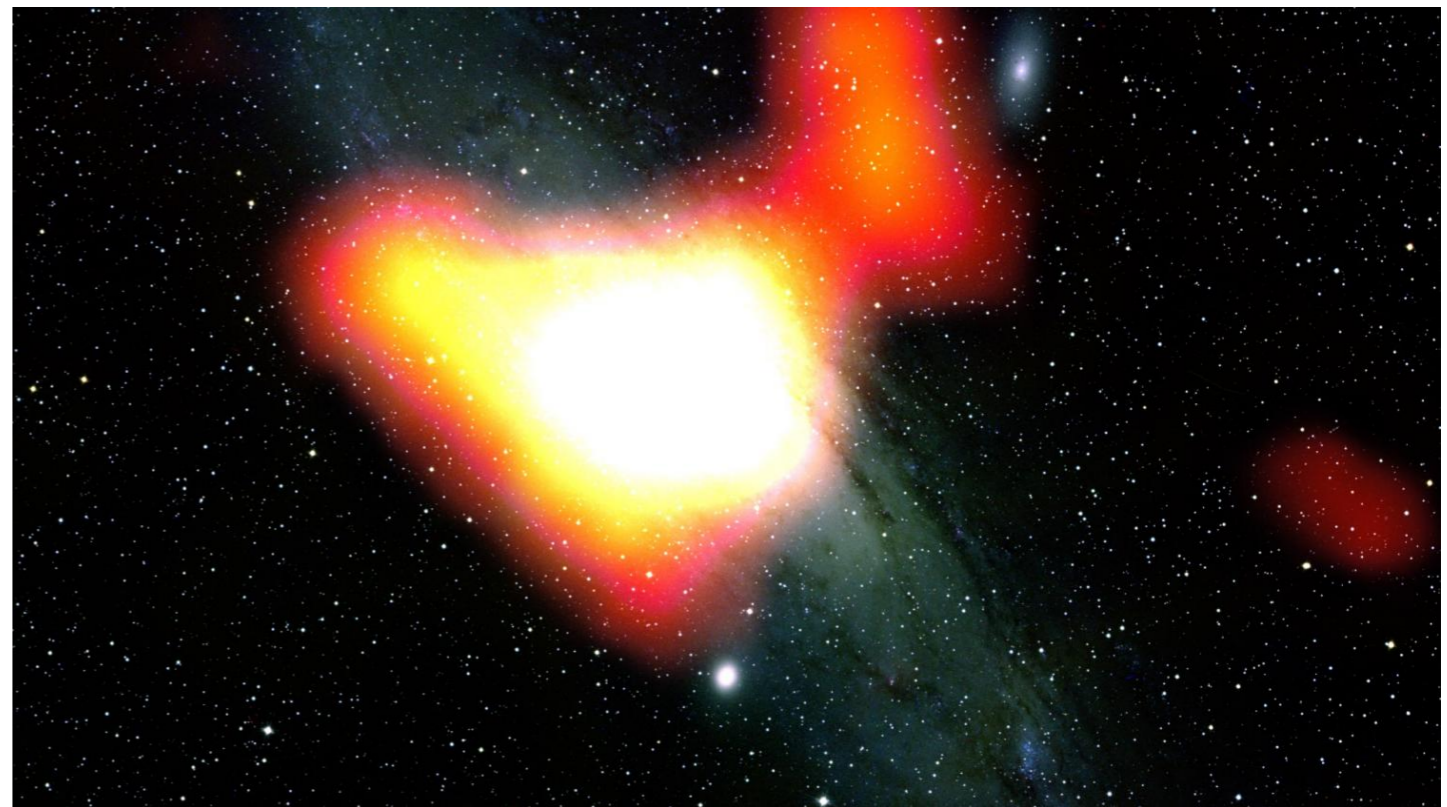
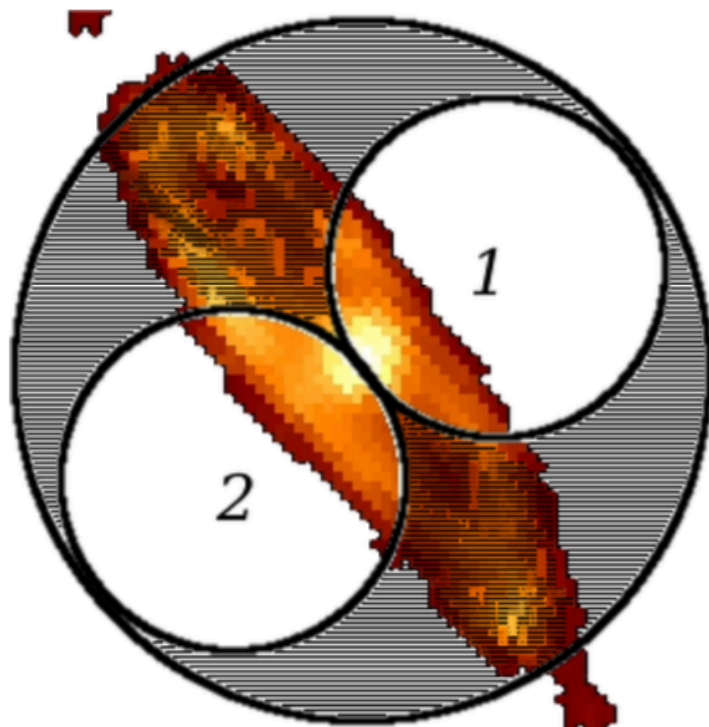
Fermi Space Telescope

Feb. 21, 2017

## Evidence of *Fermi* bubbles around M31

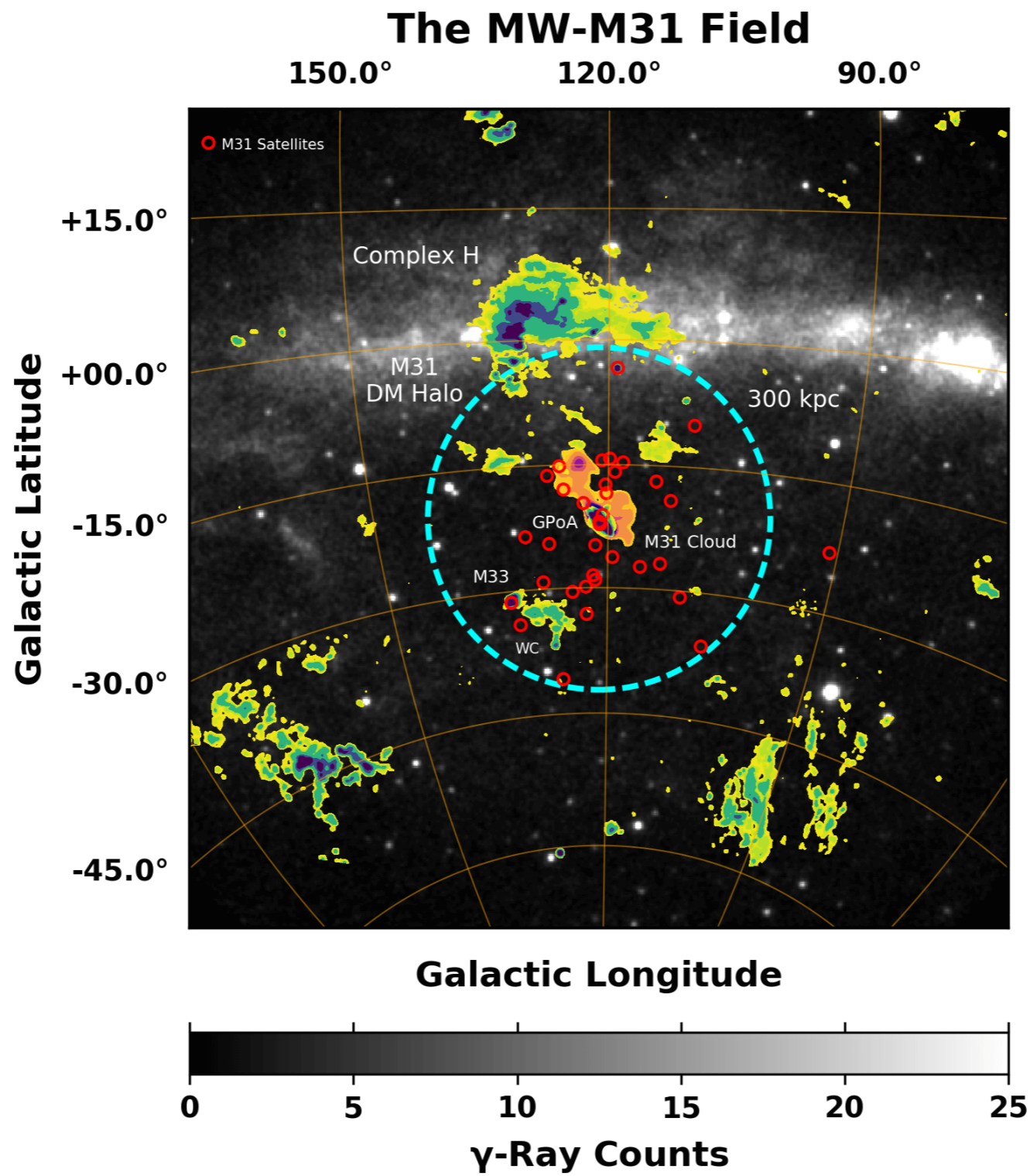
M. S. Pshirkov,<sup>1,2,3★</sup> V. V. Vasiliev<sup>4</sup> and K. A. Postnov<sup>1,5</sup>

NASA's Fermi Finds Possible Dark Matter Ties in Andromeda Galaxy

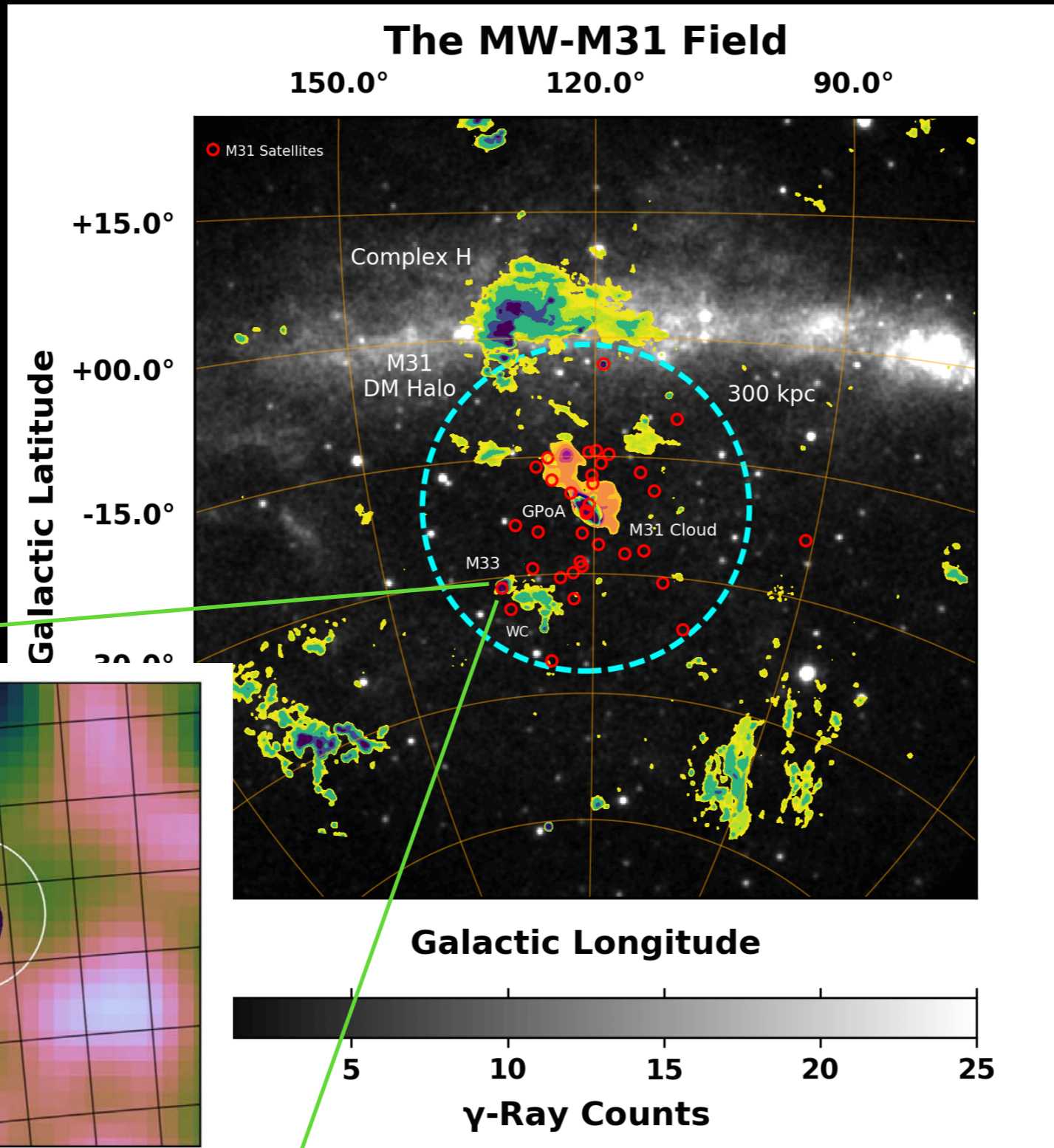


- The gamma-ray emission from M31's inner galaxy is not found to be correlated with regions rich in gas or star-formation activity.

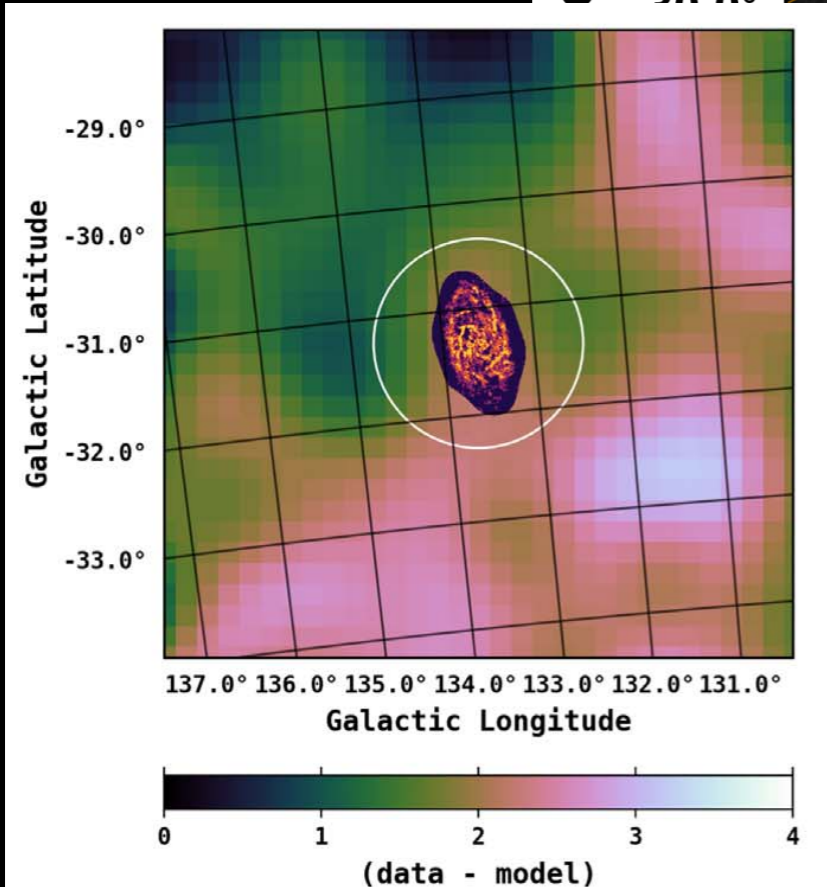
# The M31-MW Field



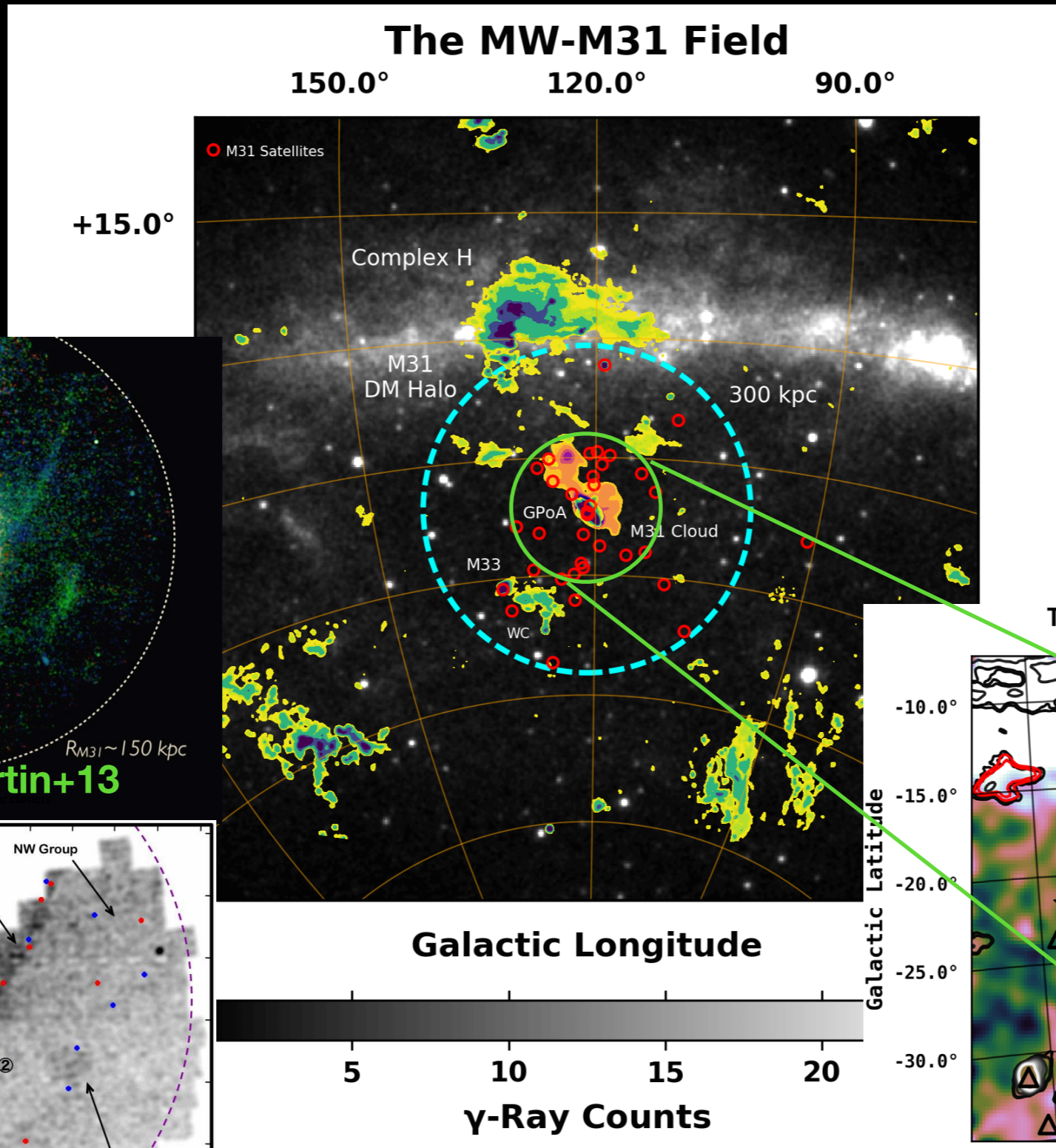
# The M31-MW Field



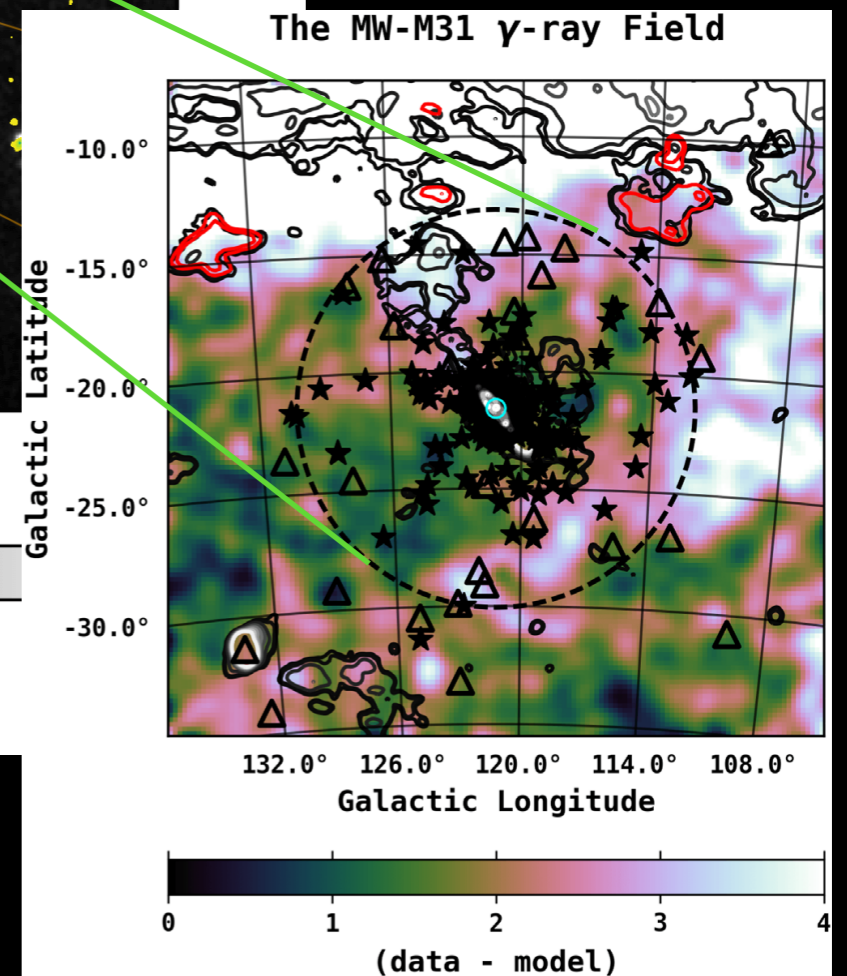
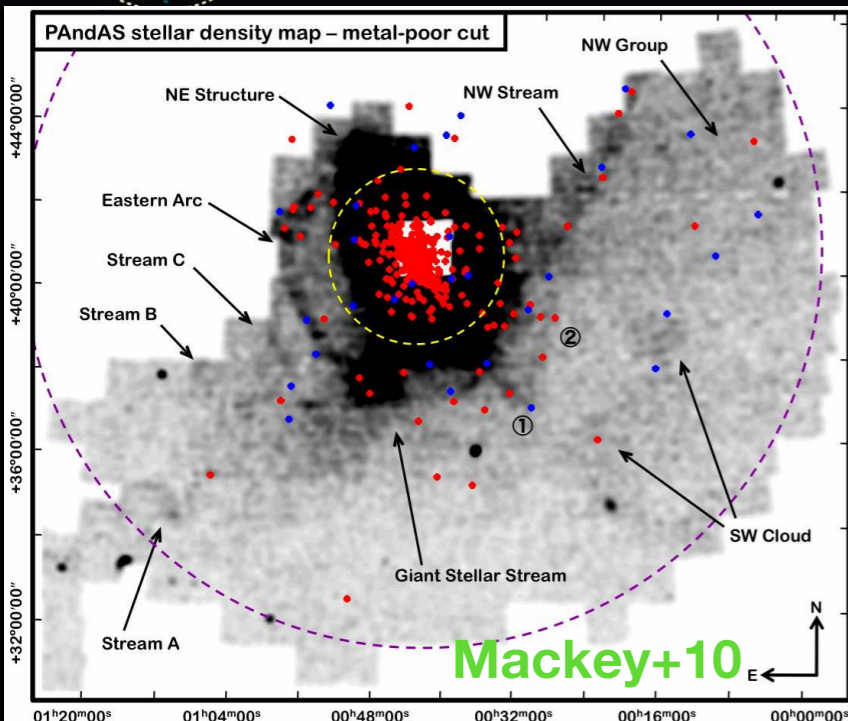
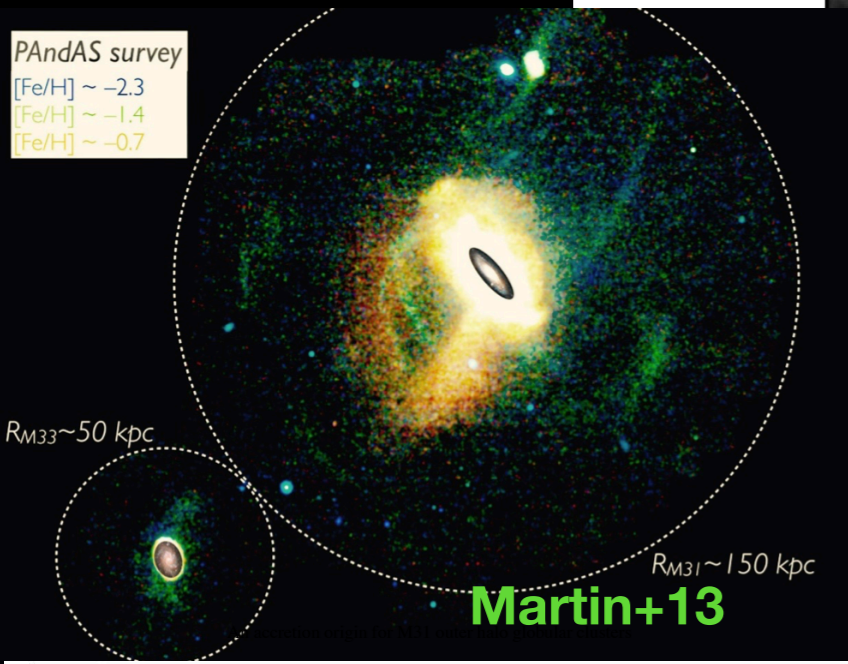
Detection of M33:  
Xi+20 and Ajello+20



# The M31-MW Field

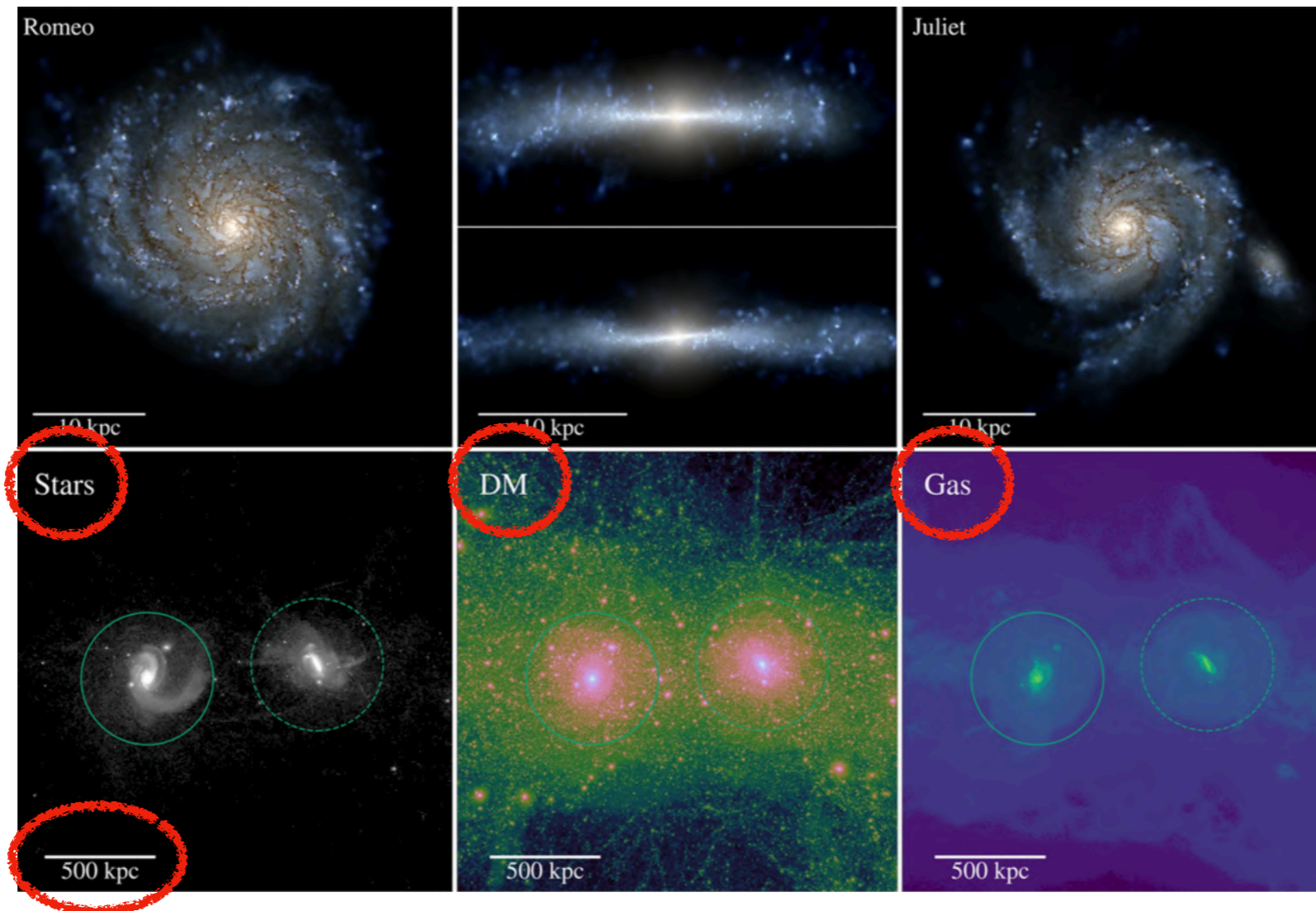


Spherical Halo  
R = 0.4 - 8.5 deg  
~120 kpc extension



# Motivation

## The big picture (illustrative)



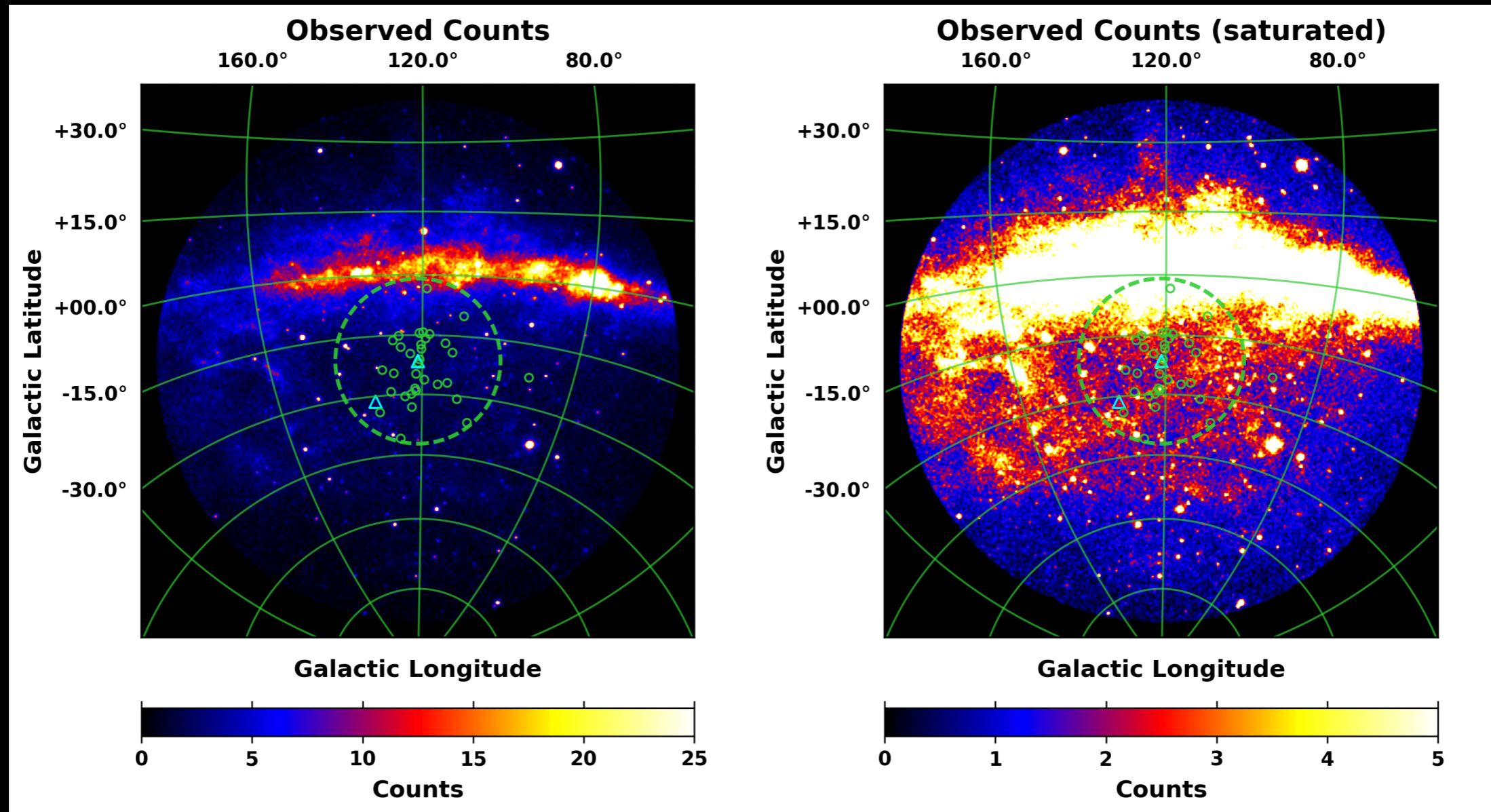
**Evidence for a  
Local Hot Bridge  
towards M31:  
Qu+21**

MW-M31-Like Pairs (for example) from Garrison-Kimmel et al. 2018 ([link](#))

- M31 harbors a massive dark matter (DM) halo which may span up to  $\sim 600$  kpc across and comprises  $\sim 90\%$  of the galaxy's total mass.
- This halo size translates into a large diameter of  $42^\circ$  on the sky for an M31-Milky Way (MW) distance of 785 kpc, but its presumably low surface brightness makes it challenging to detect with gamma-ray telescopes.
- The entire M31 DM halo is seen from the outside, so we see the extended integral signal. For the MW we see through the halo, so it can be easily confused with diffuse components.
- Line of sight ostensibly includes:  
**M31 DM halo + secondary M31 emission + local DM filament between M31 and MW + MW DM halo.**



# Fermi-LAT Observations

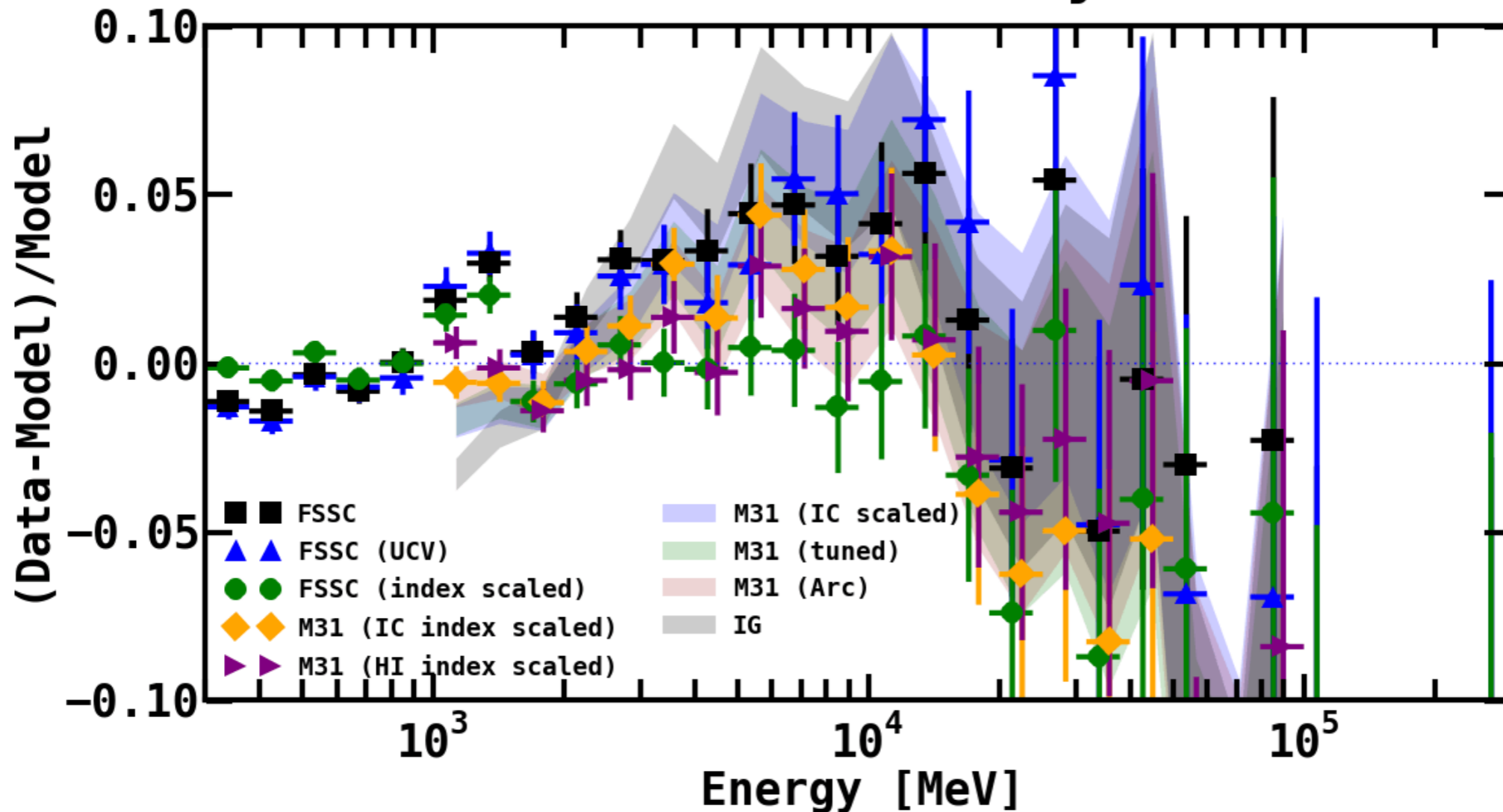


**Karwin+19, ApJ, 880, 95.**

- Data: 7.6 years (2008-08-04 to 2016-03-16)
- Full ROI is a  $60^\circ$  radius centered at the position of M31
- Energy range: 1-100 GeV in 20 bins logarithmically spaced
- left: full count range. right: saturated counts, emphasizing lower counts at high latitudes.
- Dashed green circle ( $21^\circ$  in radius) corresponds to a 300 kpc projected radius, for an M31-MW distance of 785 kpc
- M31 and M33 are shown with cyan triangles, and the rest of M31's dwarf galaxy population are shown with small green circles.

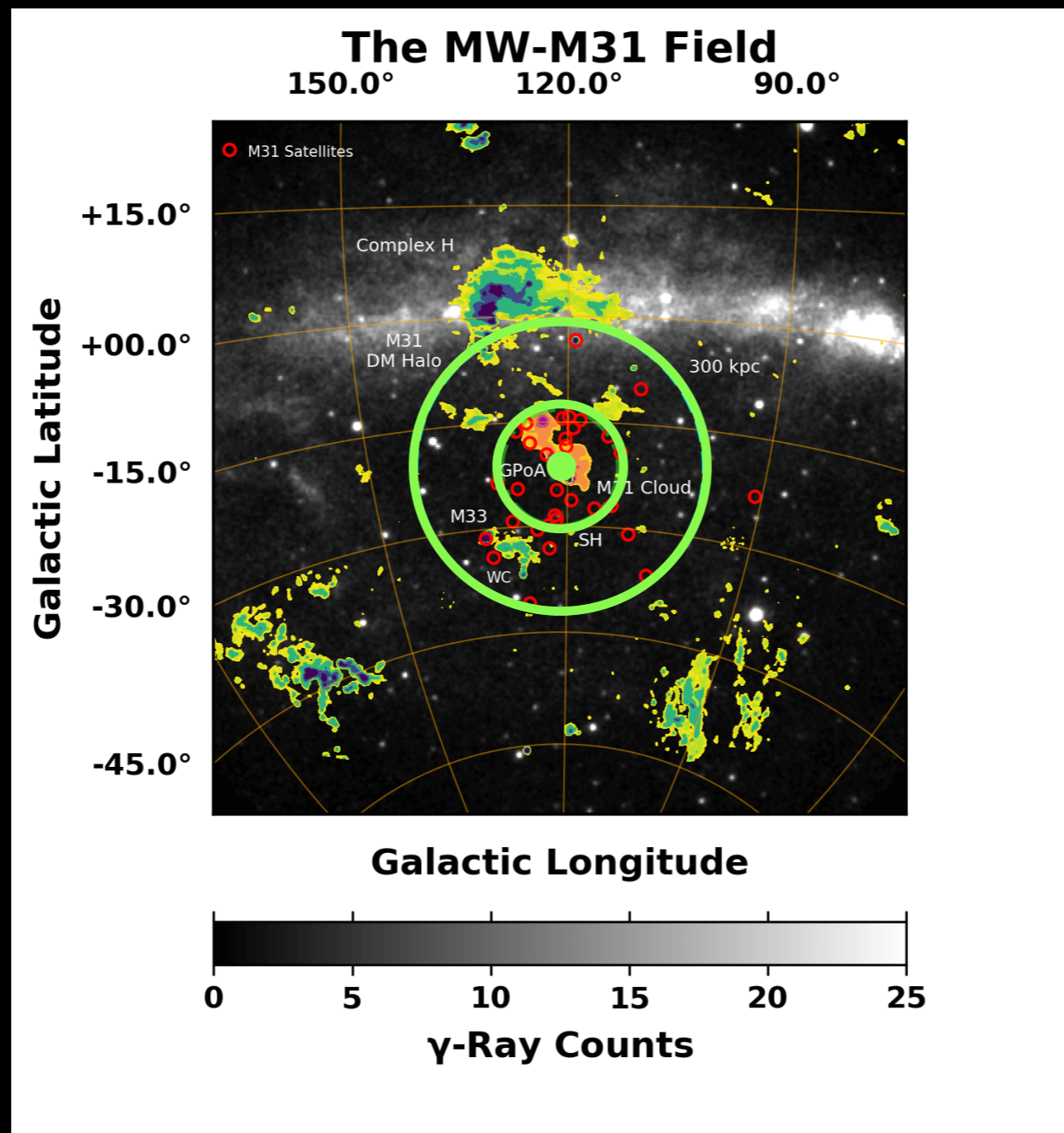
# A Systematic Excess

## Statistical ( $1\sigma$ ) + Systematic



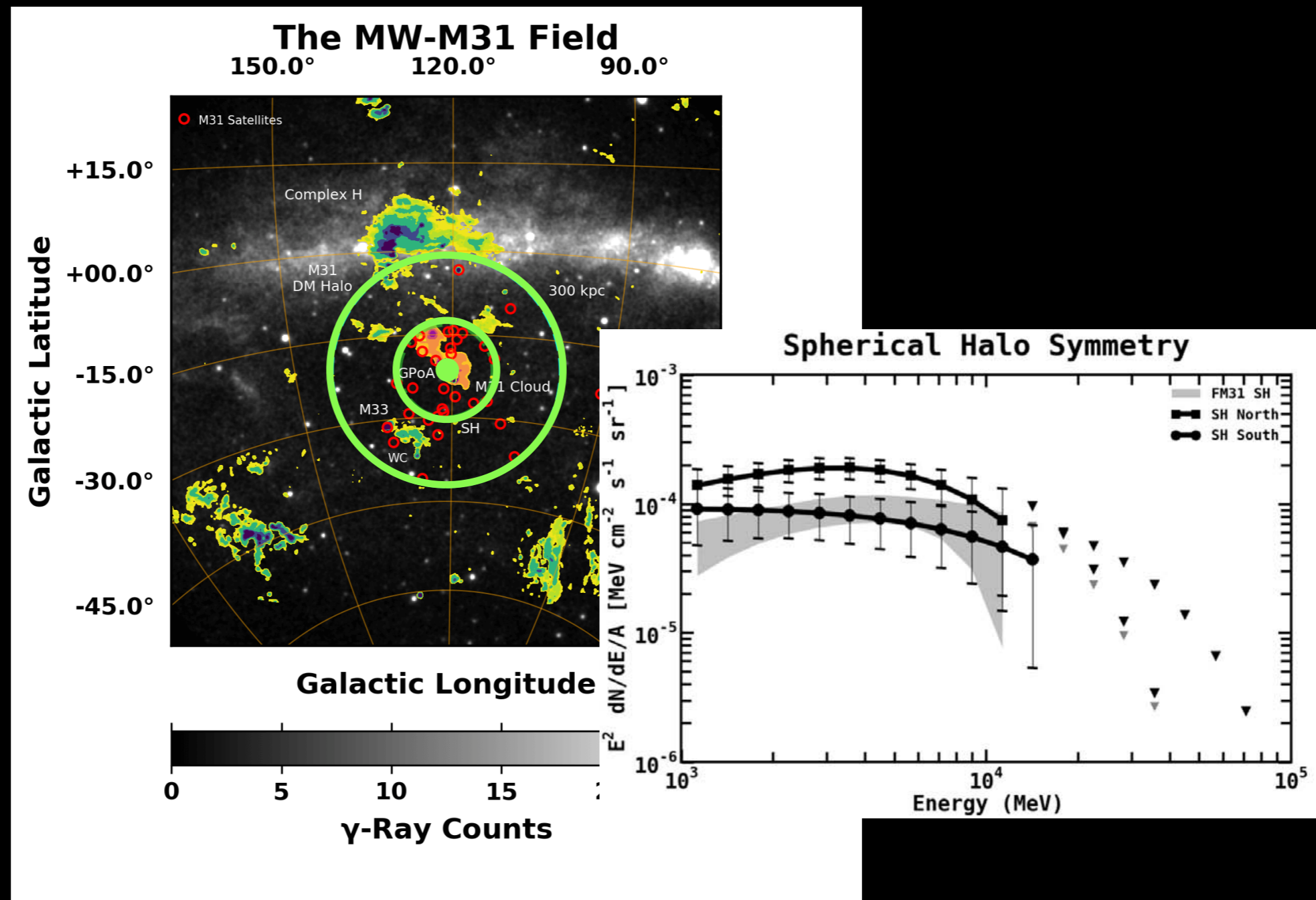
- We perform 9 main variations of the fit, using 3 different IEMs.
- We conclude that a systematic excess is present between  $\sim 3$ -20 GeV at the level of  $\sim 3$ -5%.
- Our analysis shows that the characterization of the HI-related emission along the line of sight is a significant systematic uncertainty for observations towards M31's outer halo. All models we have tested use similar underlying HI maps. This will be fully addressed in a forthcoming work.

# The M31 System



- We characterize the M31 system with three concentric templates.
- Inner galaxy (IG): 0.4 degree disk.
- Spherical halo (SH): ring from 0.4 - 8.5 degree, corresponding to a projected radius of  $\sim 120$  kpc.
- Far outer halo (FOH): extending from 8.5 degrees, covering the remaining field.

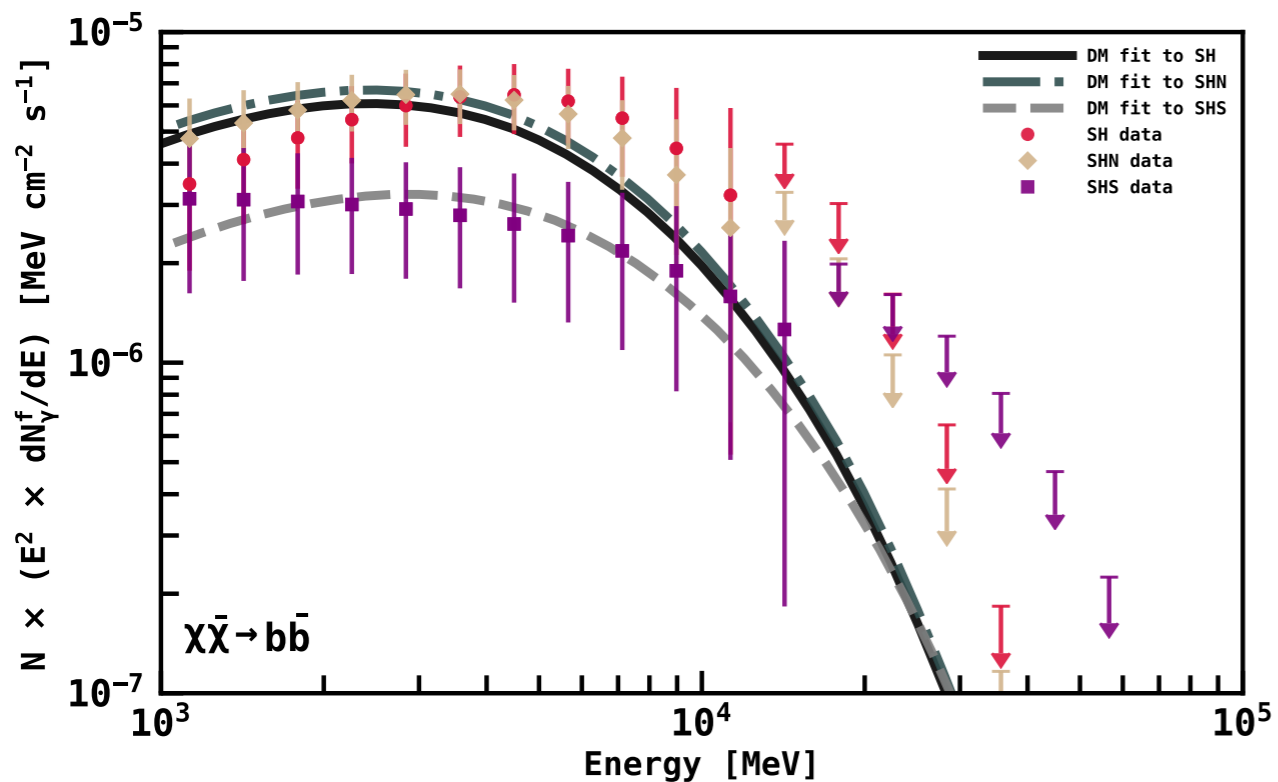
# The M31 System



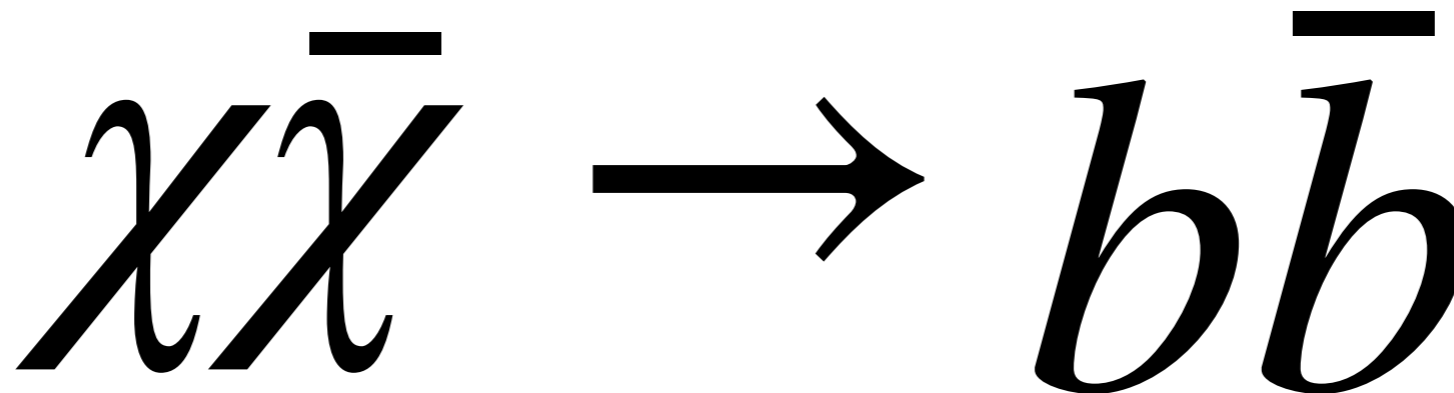
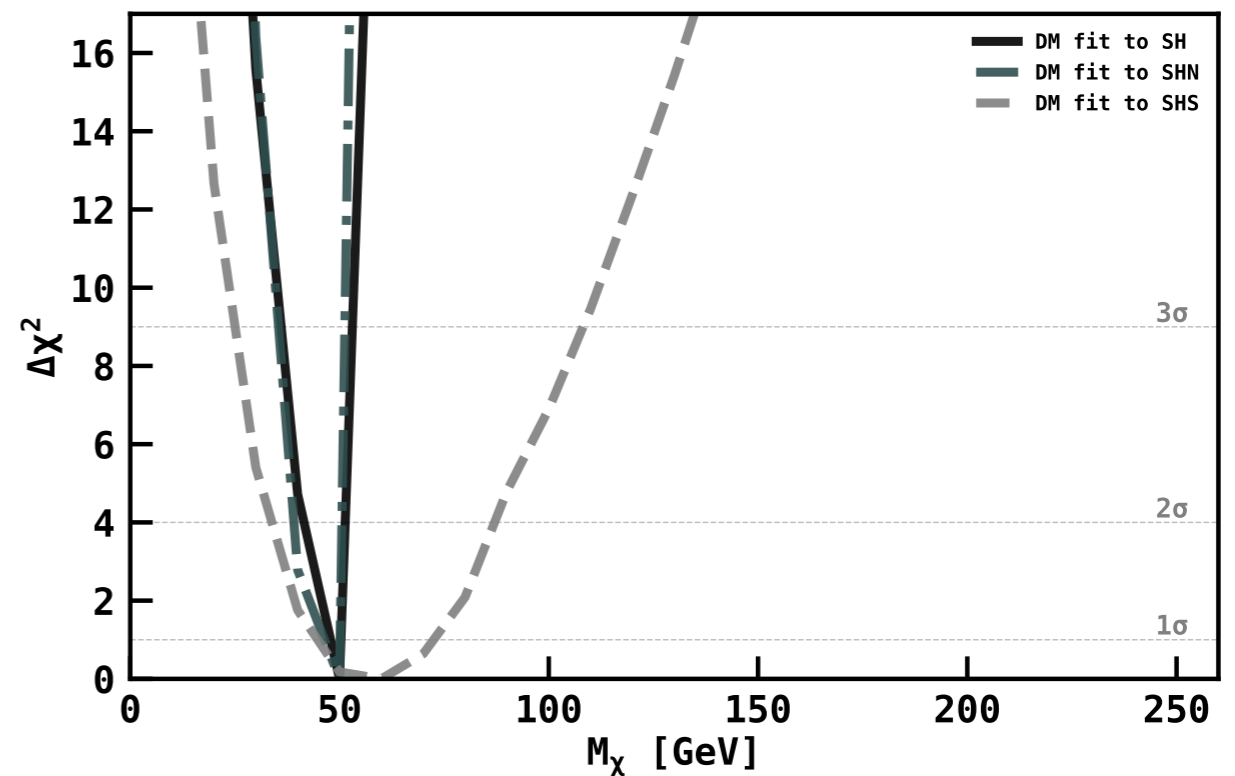
- We characterize the M31 system with three concentric templates.
- Inner galaxy (IG): 0.4 degree disk.
- Spherical halo (SH): ring from 0.4 - 8.5 degree, corresponding to a projected radius of  $\sim 120$  kpc.
- Far outer halo (FOH): extending from 8.5 degrees, covering the remaining field.

# DM Fit (Mass)

DM Flux



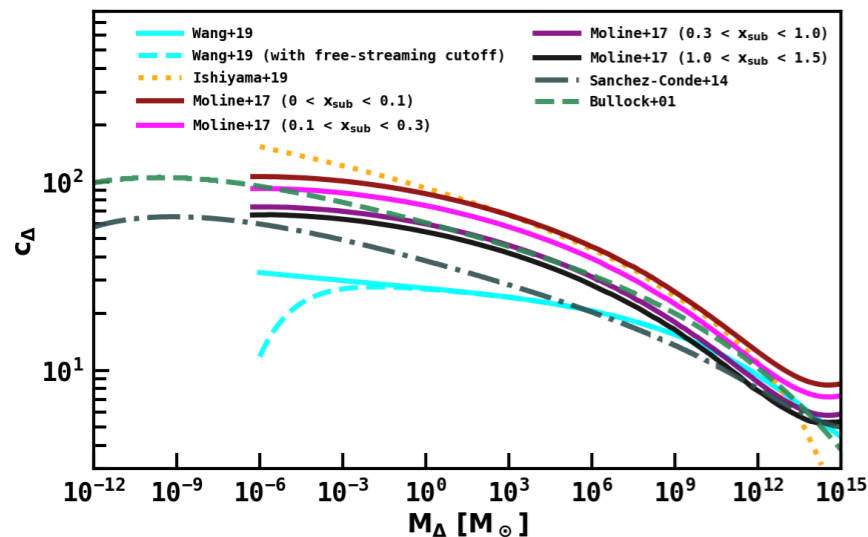
DM Mass



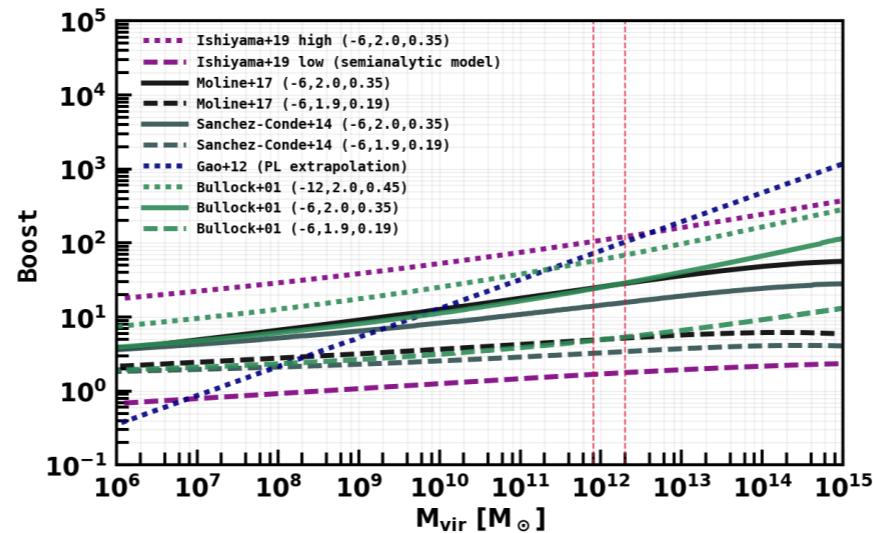
- The best-fit spectra are shown in the left plot.
- The right plot shows the profile for the three different fit variations. The best-fit mass for the SH and SHN model is  $\sim 50$  GeV. The best fit mass for the SHS model is  $\sim 60$  GeV.
- Dashed grey lines show the 1,2, and 3 sigma contours, for 1 degree of freedom.

# Determining the J-Factor

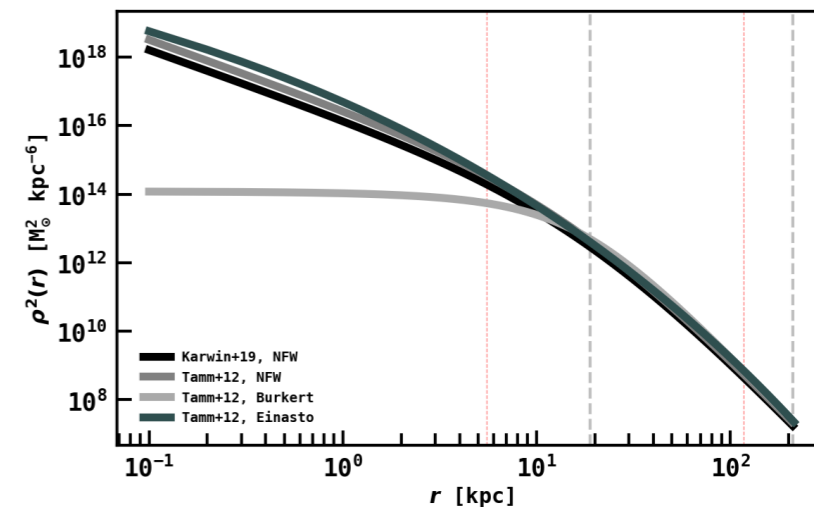
$c_{\Delta}$ - $M_{\Delta}$  Relations



Boost Factor



DM Density Profile



$$B(M) = \frac{4 \pi R_{200}^3}{\mathcal{L}_{\text{smooth}}(M)} \int_{M_{\text{min}}}^M dm \int_0^1 dx_{\text{sub}} \times \frac{dn(m, x_{\text{sub}})}{dm} \mathcal{L}(m, x_{\text{sub}}) x_{\text{sub}}^2,$$

$$\mathcal{L}_{\text{smooth}}(M) \equiv \int_0^{R_{200}} \rho_{\text{host}}^2(r) 4 \pi r^2 dr$$

$$= \frac{M c_{200}^h(M)^3}{[f(c_{200}^h(M))]^2} \frac{200 \rho_c}{9} \left( 1 - \frac{1}{(1 + c_{200}^h(M))^3} \right)$$

$$\mathcal{L}(m, x_{\text{sub}}) = [1 + B(m, x_{\text{sub}})] \mathcal{L}_{\text{smooth}}(m, x_{\text{sub}}),$$

(Moline+17)

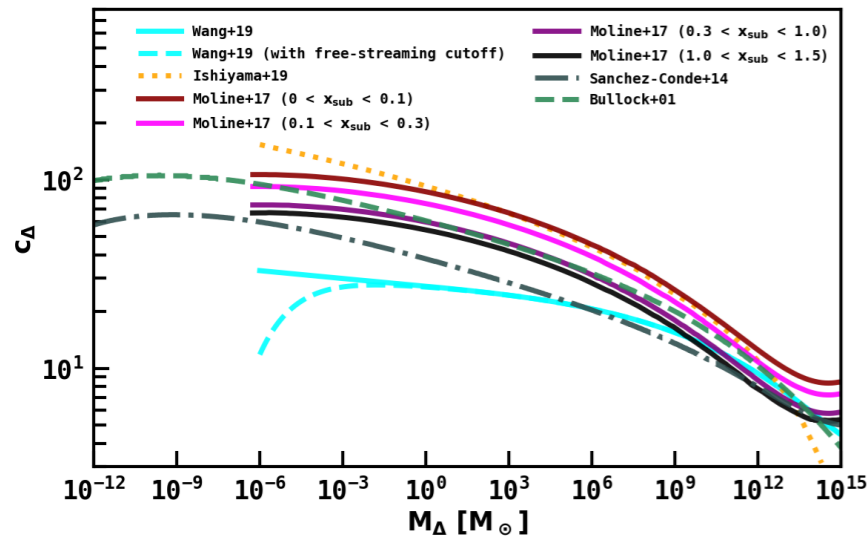
## The main parameters for the boost factor:

- minimum subhalo mass:  $1e-6 - 1e6 M_{\text{sun}}$
- subhalo mass function (index; normalization): 1.9, 2.0; 0.12, 0.35.
- mass-concentration relationship: Moline+17
- mass distribution of subhalos: same as main halo (NFW and Einasto)
- distribution of subhalos in main halo: same as main halo (NFW and Einasto)
- We consider 2 levels of substructure.
- Total boost factor ranges from  $\sim 1.5-26$

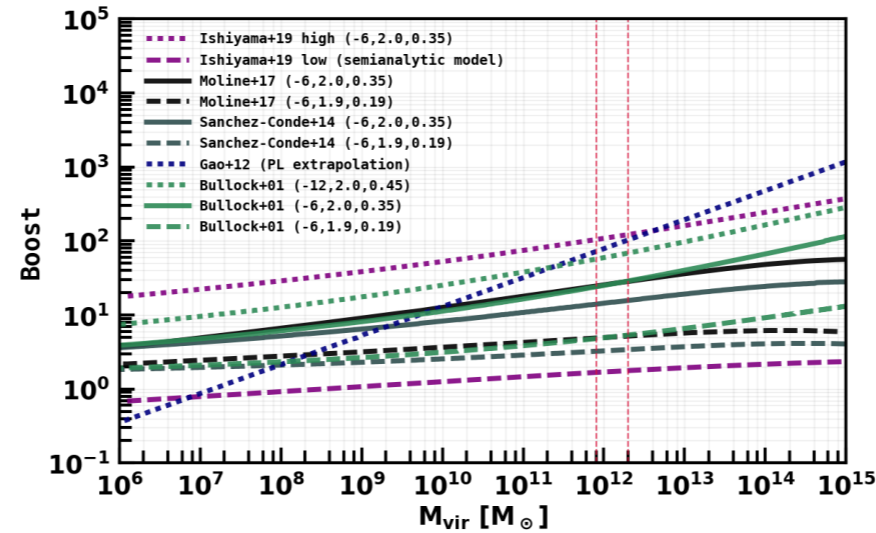
**\*J-factors are calculated with CLUMPY**

# Determining the J-Factor

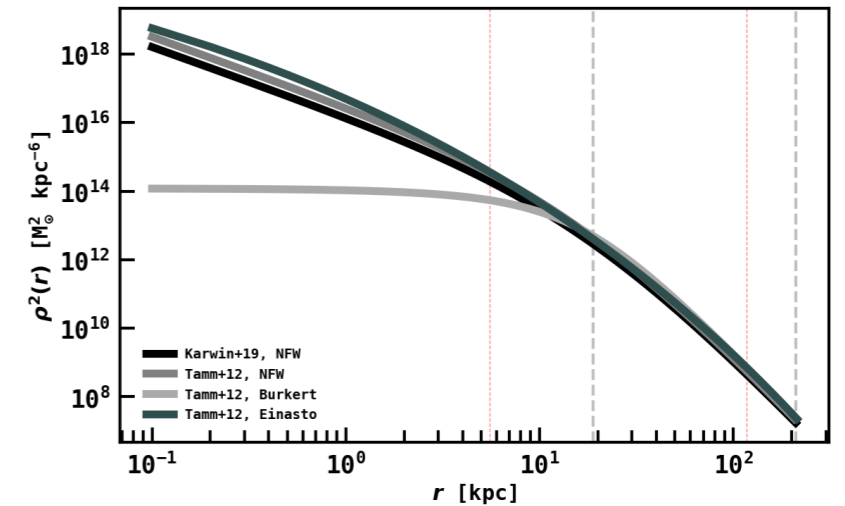
$c_{\Delta}$ - $M_{\Delta}$  Relations



Boost Factor



DM Density Profile



$$B(M) = \frac{4 \pi R_{200}^3}{\mathcal{L}_{\text{smooth}}(M)} \int_{M_{\min}}^M dm \int_0^1 dx_{\text{sub}} \times \frac{dn(m, x_{\text{sub}})}{dm} \mathcal{L}(m, x_{\text{sub}}) x_{\text{sub}}^2,$$

$$\mathcal{L}_{\text{smooth}}(M) \equiv \int_0^{R_{200}} \rho_{\text{host}}^2(r) 4 \pi r^2 dr$$

$$= \frac{M c_{200}^h(M)^3}{[f(c_{200}^h(M))]^2} \frac{200 \rho_c}{9} \left( 1 - \frac{1}{(1 + c_{200}^h(M))^3} \right)$$

$$\mathcal{L}(m, x_{\text{sub}}) = [1 + B(m, x_{\text{sub}})] \mathcal{L}_{\text{smooth}}(m, x_{\text{sub}}),$$

(Moline+17)

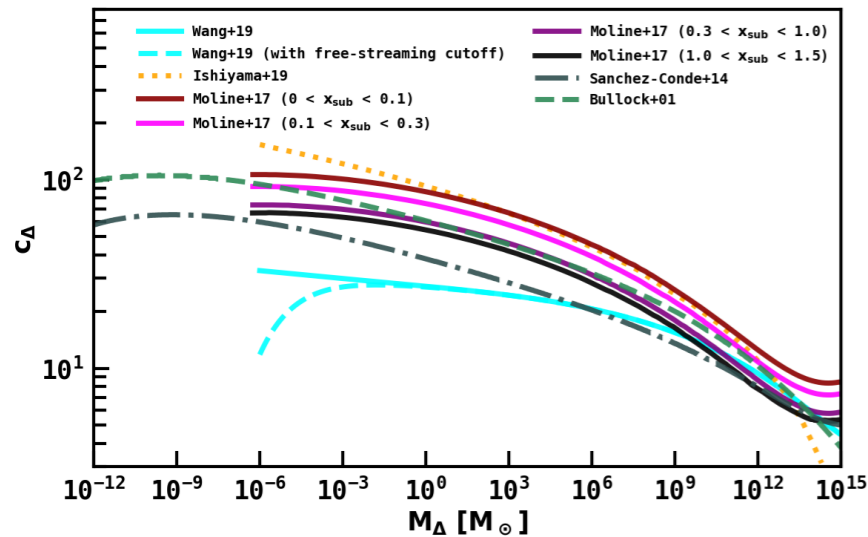
## The main parameters for the boost factor:

- minimum subhalo mass:  $1e-6 - 1e6 M_{\text{sun}}$
- subhalo mass function (index; normalization): 1.9, 2.0; 0.12, 0.35.
- mass-concentration relationship: Moline+17
- mass distribution of subhalos: same as main halo (NFW and Einasto)
- distribution of subhalos in main halo: same as main halo (NFW and Einasto)
- We consider 2 levels of substructure.
- Total boost factor ranges from  $\sim 1.5-26$

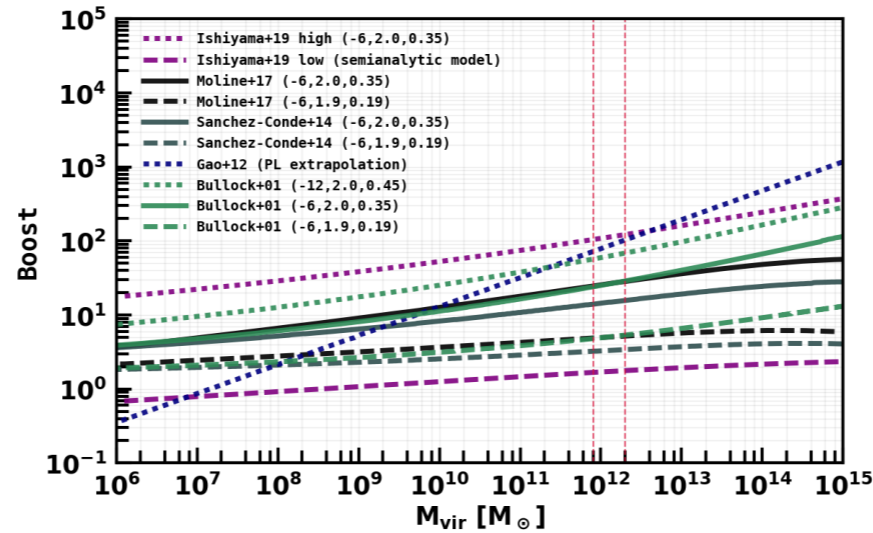
**\*J-factors are calculated with CLUMPY**

# Determining the J-Factor

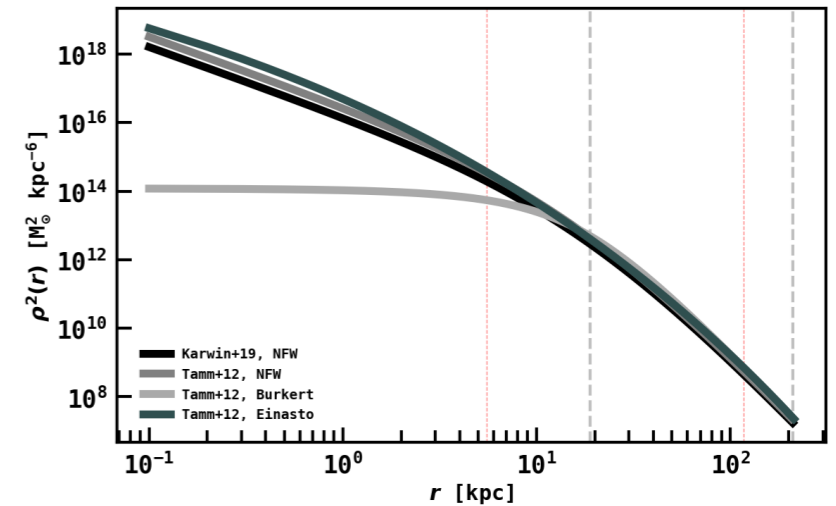
$c_{\Delta}$ - $M_{\Delta}$  Relations



Boost Factor



DM Density Profile



$$B(M) = \frac{4 \pi R_{200}^3}{\mathcal{L}_{\text{smooth}}(M)} \int_{M_{\min}}^M dm \int_0^1 dx_{\text{sub}} \times \frac{dn(m, x_{\text{sub}})}{dm} \mathcal{L}(m, x_{\text{sub}}) x_{\text{sub}}^2,$$

$$\mathcal{L}_{\text{smooth}}(M) \equiv \int_0^{R_{200}} \rho_{\text{host}}^2(r) 4 \pi r^2 dr$$

$$= \frac{M c_{200}^h(M)^3}{[f(c_{200}^h(M))]^2} \frac{200 \rho_c}{9} \left( 1 - \frac{1}{(1 + c_{200}^h(M))^3} \right)$$

$$\mathcal{L}(m, x_{\text{sub}}) = [1 + B(m, x_{\text{sub}})] \mathcal{L}_{\text{smooth}}(m, x_{\text{sub}}),$$

(Moline+17)

## The main parameters for the boost factor:

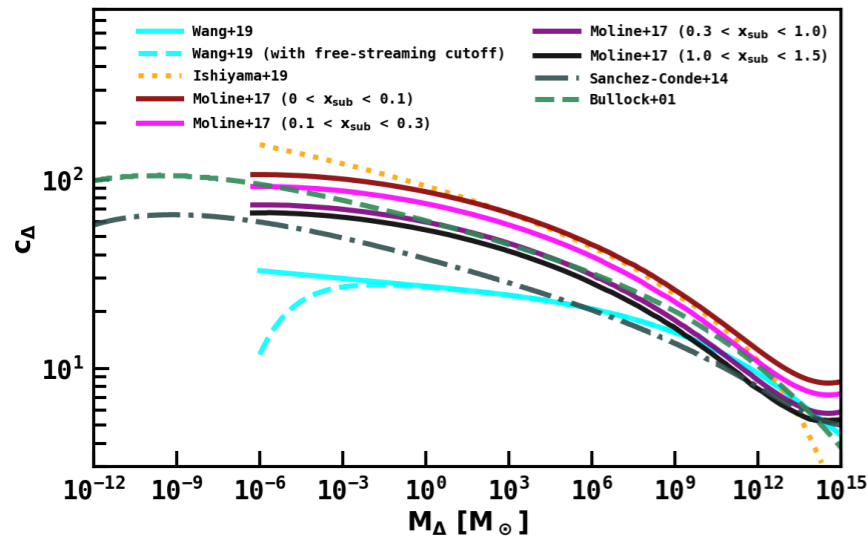
- minimum subhalo mass:  $1e-6 - 1e6 M_{\text{sun}}$
- subhalo mass function (index; normalization): 1.9, 2.0; 0.12, 0.35.
- mass-concentration relationship: Moline+17
- mass distribution of subhalos: same as main halo (NFW and Einasto)
- distribution of subhalos in main halo: same as main halo (NFW and Einasto)
- We consider 2 levels of substructure.
- Total boost factor ranges from  $\sim 1.5-26$

**\*J-factors are calculated with CLUMPY**

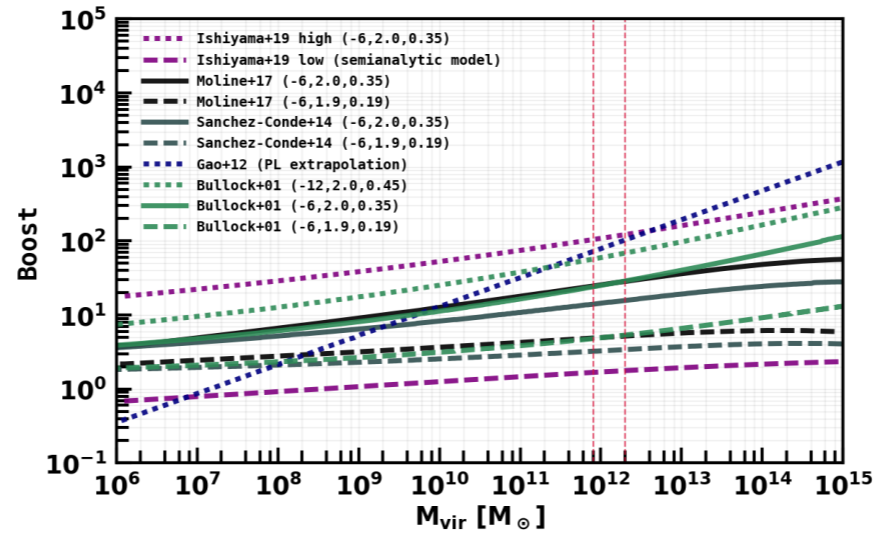


# Determining the J-Factor

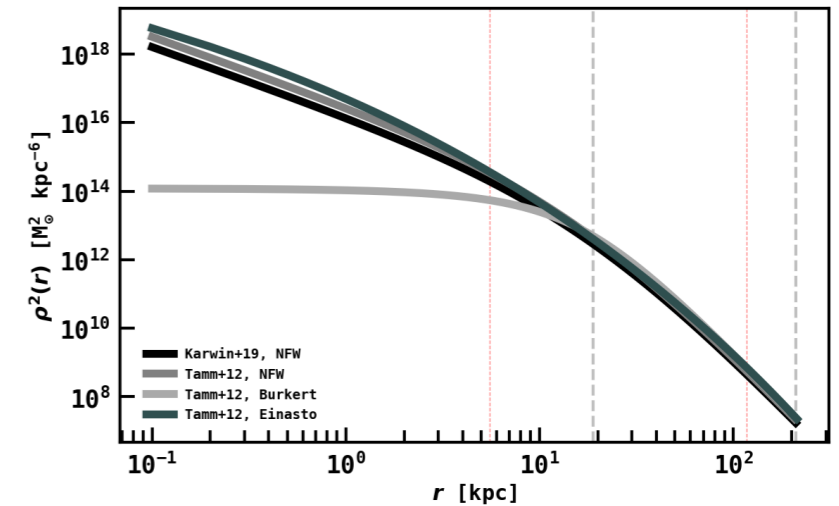
$c_{\Delta}$ - $M_{\Delta}$  Relations



Boost Factor



DM Density Profile



$$B(M) = \frac{4 \pi R_{200}^3}{\mathcal{L}_{\text{smooth}}(M)} \int_{M_{\text{min}}}^M dm \int_0^1 dx_{\text{sub}} \times \frac{dn(m, x_{\text{sub}})}{dm} \mathcal{L}(m, x_{\text{sub}}) x_{\text{sub}}^2,$$

$$\begin{aligned} \mathcal{L}_{\text{smooth}}(M) &\equiv \int_0^{R_{200}} \rho_{\text{host}}^2(r) 4 \pi r^2 dr \\ &= \frac{M c_{200}^h(M)^3}{[f(c_{200}^h(M))]^2} \frac{200 \rho_c}{9} \left( 1 - \frac{1}{(1 + c_{200}^h(M))^3} \right) \end{aligned}$$

$$\mathcal{L}(m, x_{\text{sub}}) = [1 + B(m, x_{\text{sub}})] \mathcal{L}_{\text{smooth}}(m, x_{\text{sub}}),$$

(Moline+17)

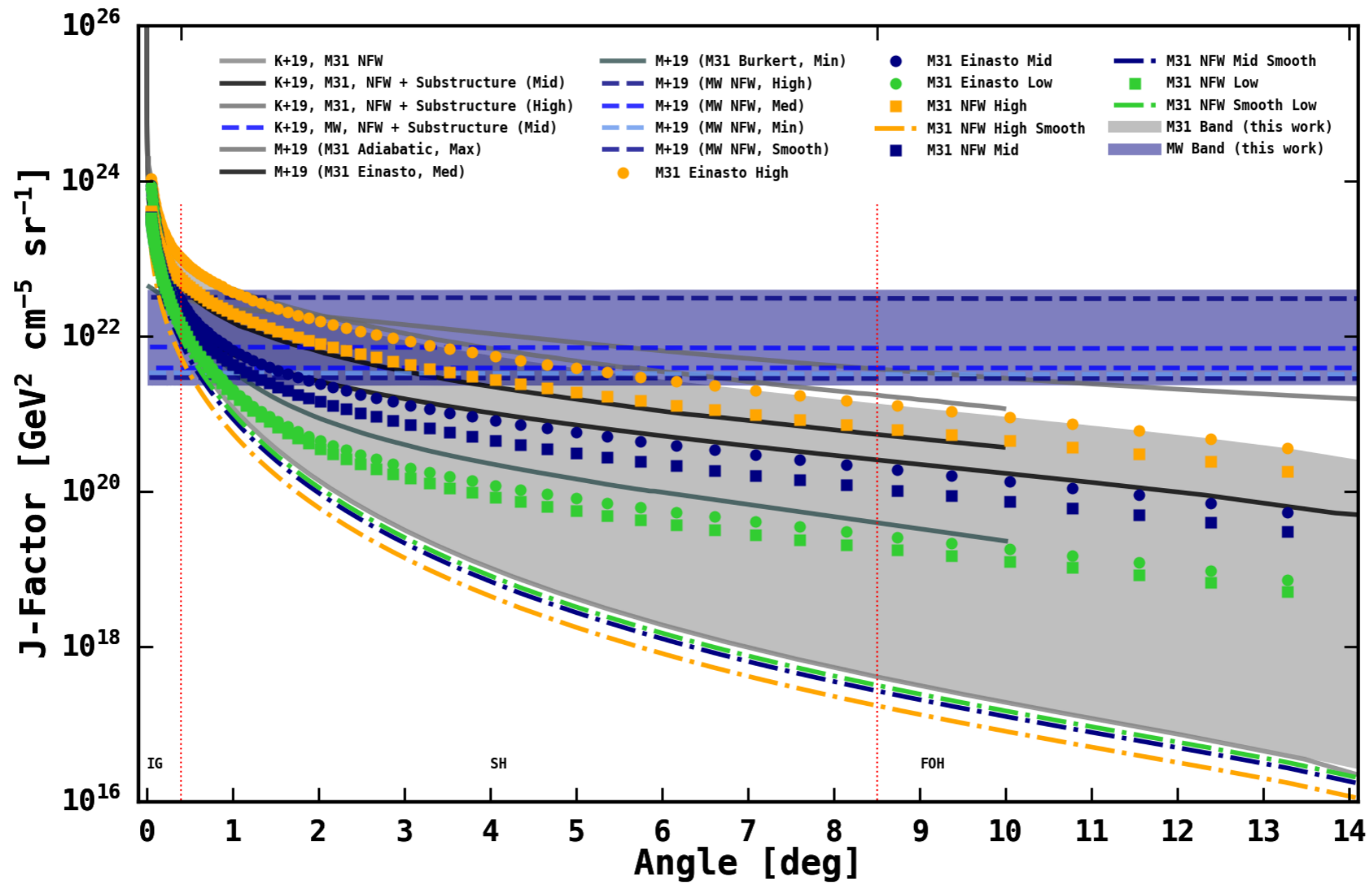
## The main parameters for the boost factor:

- minimum subhalo mass:  $1e-6 - 1e6 M_{\text{sun}}$
- subhalo mass function (index; normalization): 1.9, 2.0; 0.12, 0.35.
- mass-concentration relationship: Moline+17
- mass distribution of subhalos: same as main halo (NFW and Einasto)
- distribution of subhalos in main halo: same as main halo (NFW and Einasto)
- We consider 2 levels of substructure.
- Total boost factor ranges from  $\sim 1.5-26$

**\*J-factors are calculated with CLUMPY**

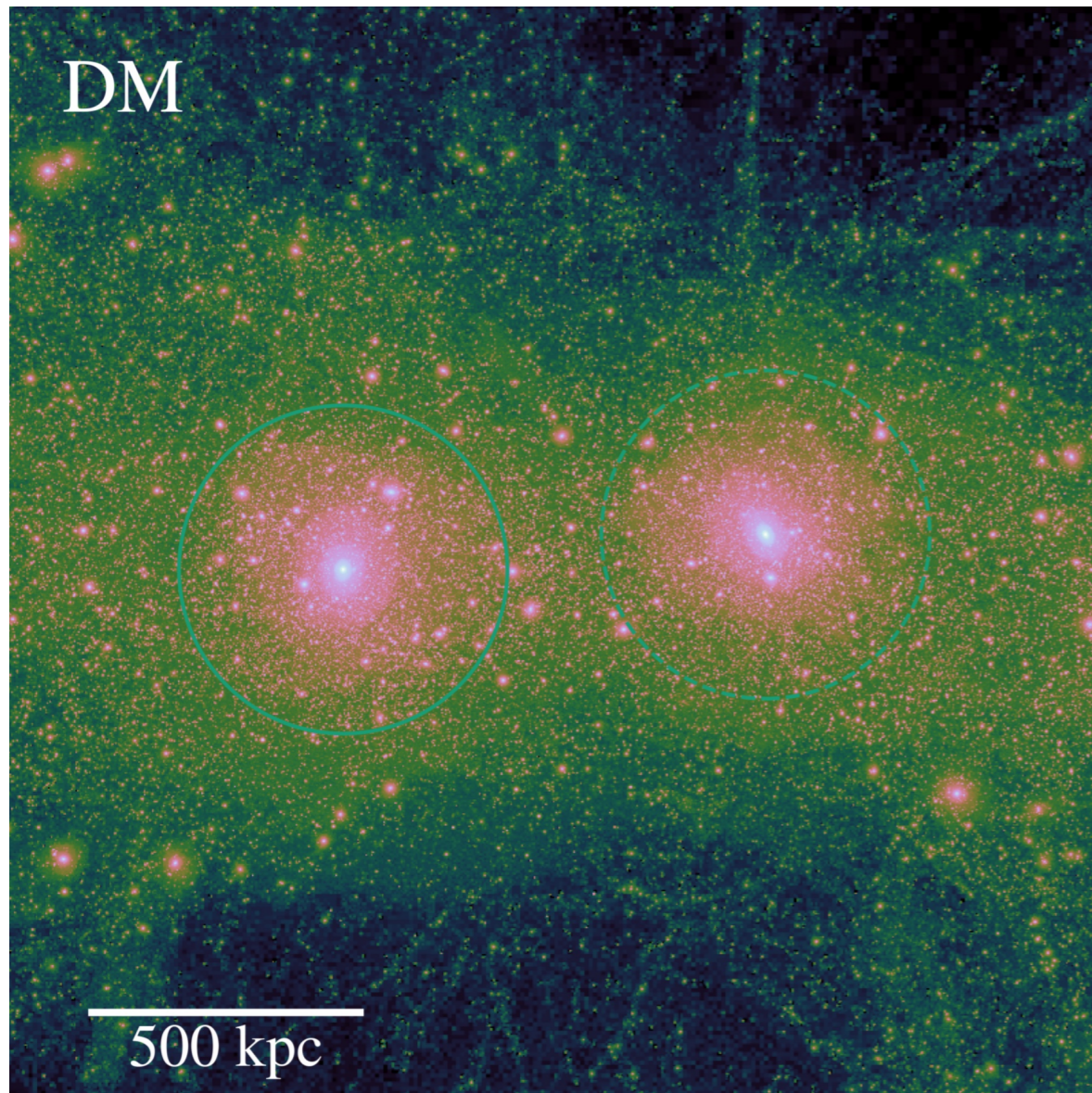
# J-Factor Uncertainty

## FM31 J-Factor



- Grey band is the J-factor uncertainty for M31 from this work.
- Purple band is the J-factor uncertainty for the MW from this work.
- Markers are the M31 calculations for the NFW (squares) and Einasto (circles) profiles, with the boost factor.

# Observing M31's DM Halo from Inside the MW's DM Halo



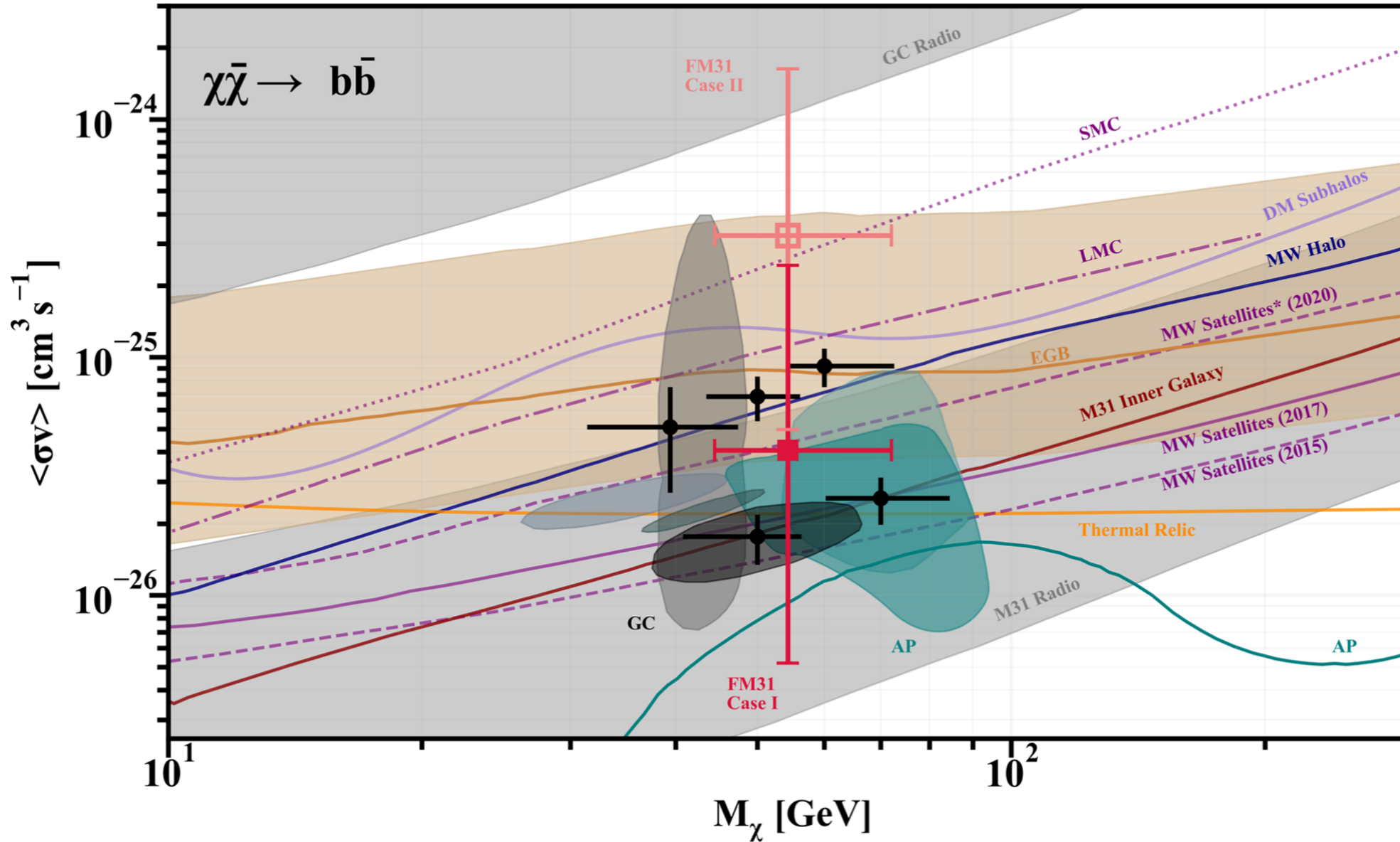
MW-M31-Like Pairs (for example) from Garrison-Kimmel et al. 2018 ([link](#))

## Contribution from the MW's DM halo along LOS:

- This observational uncertainty is quantified by considering the two extreme cases.
- Case I:  $J_{\text{total}} = J_{\text{M31}} + J_{\text{MW}}$
- Case II:  $J_{\text{total}} = J_{\text{M31}}$

# DM Parameter Space

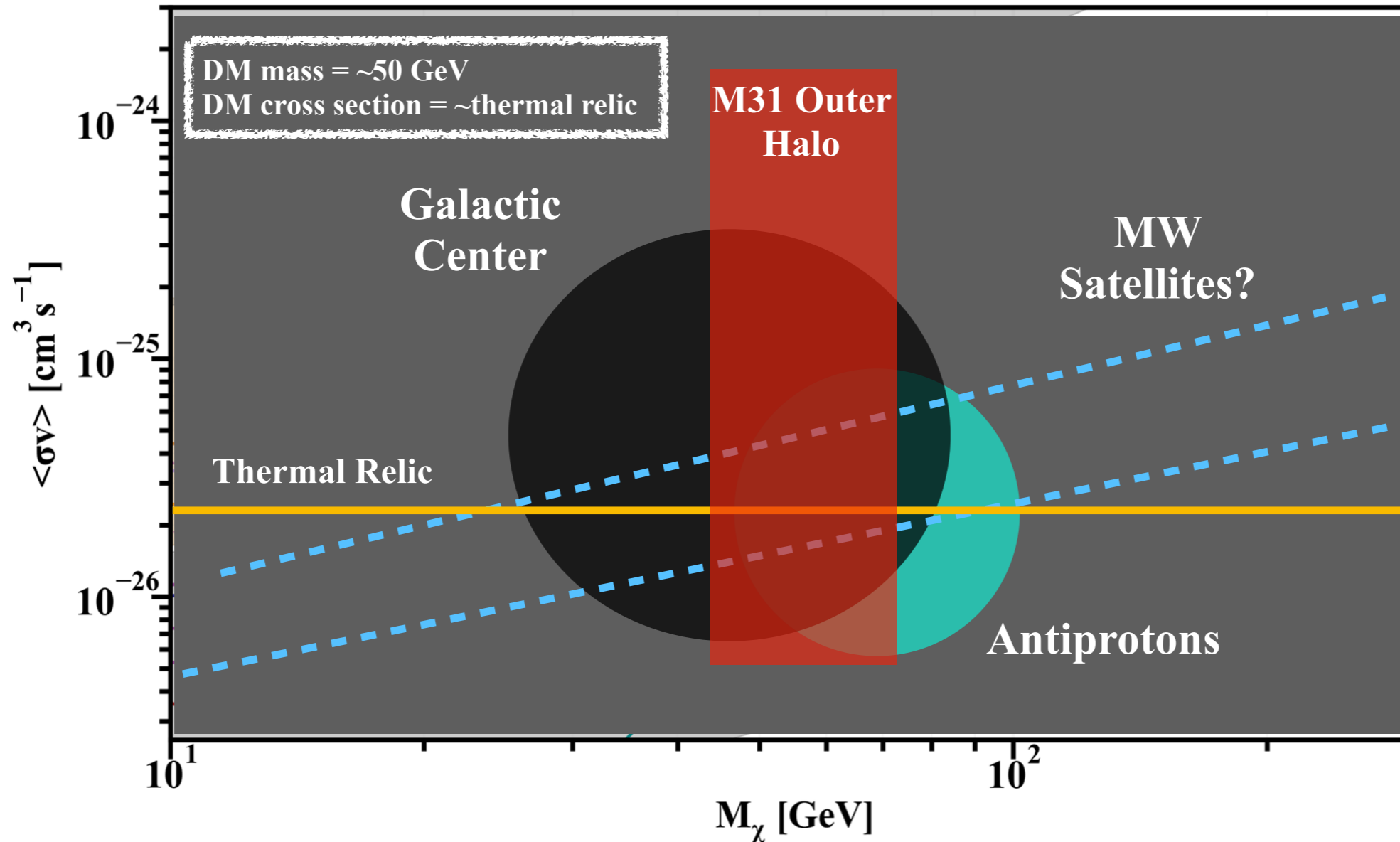
## DM Indirect Detection



- Legend
- |                                       |  |                                      |
|---------------------------------------|--|--------------------------------------|
| — Thermal Relic, Steigman et al. 2012 | ■ AP, Cuoco et al. 2017                | — LMC, Buckley et al. 2015           |
| ■ GC, Gordon & Macias 2013            | — AP, Reinert et al. 2018              | ⋯ SMC, Caputo et al. 2016            |
| ● GC, Abazajian et al. 2014           | ■ AP, Cholis et al. 2019               | — DM Subhalos, Hooper & Witte 2017   |
| ■ GC, Calore et al. 2015              | — MW Halo, Ackermann et al. 2012       | ■ GC Radio, Cholis et al. 2015       |
| ■ GC, Daylan et al. 2016              | — EGB, Ajello et al. 2015              | ■ M31 Radio, Egorov & Pierpaoli 2013 |
| ■ GC, Abazajian & Keeley 2016         | — MW Satellites, Ackermann et al. 2015 | — M31 IG, Di Mauro et al. 2019       |
| ● GC, Karwin et al. 2017 (Pulsars)    | — MW Satellites, Albert et al. 2017    | ■ FM31 (MW+M31 mid)                  |
| ● GC, Karwin et al. 2017 (OB Stars)   | — MW Satellites*, Ando et al. 2020     | □ FM31 (M31 mid)                     |

# DM Parameter Space

## DM Indirect Detection



- What is the true extension/morphology of M31 gamma-ray emission?
- millisecond pulsars?
- CR halo + circumgalactic gas?
- Outflows (Recchia+21, Ajello+21)?

# Conclusions

---

- The observed excess favors a DM particle with a mass of  $\sim 46-73$  GeV.
- The full systematic uncertainty in the cross-section currently spans 2.5 orders of magnitude, ranging from  $8e-27 - 4e-24$  cm<sup>3</sup>/s.
- This large uncertainty is due to two main factors, namely, an uncertainty in the subhalo nature and geometry of the DM halos for both M31 and the MW, and correspondingly, an uncertainty in the contribution from the MW's DM halo along the line of sight.
- Under the assumption that the minimum subhalo mass is at least  $\sim 1e-6 M_{\text{sun}}$  and the contribution from the MW's DM halo along the line-of-sight is at least  $\sim 30\%$  its total value, we show that there is a large overlap with the DM interpretations of both the GC excess and the antiproton excess, while also being compatible with the limits for the MW dwarfs.
- Although the uncertainty in the current measurements is clearly far too large to make any robust conclusions (either positive or negative), we identify a region in parameter space that still remains viable for the discovery of the DM particle.

Thank you!